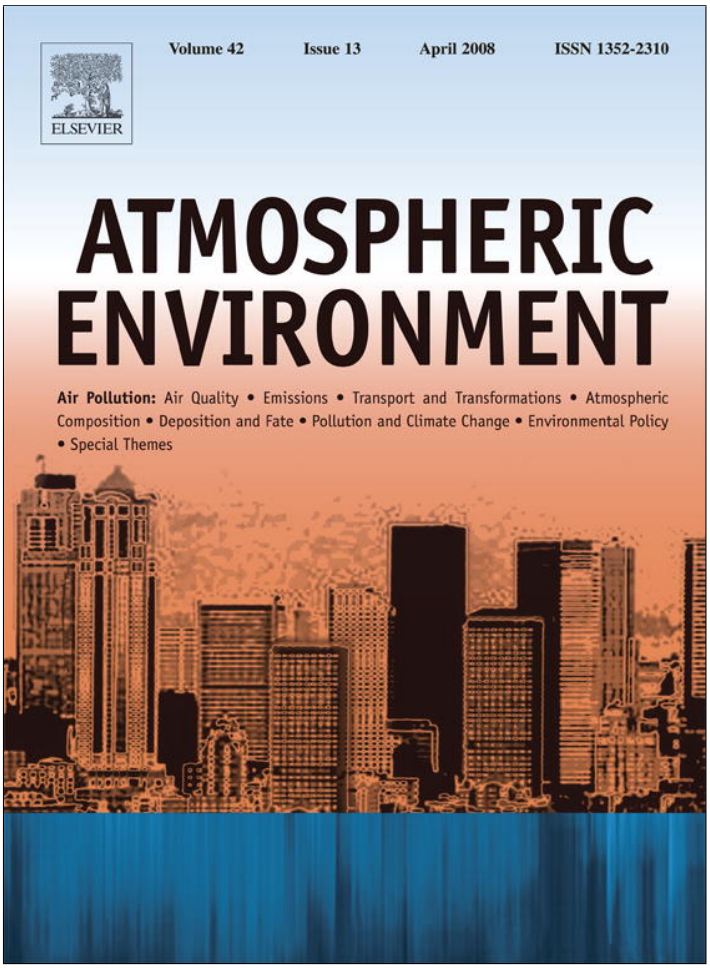

Available online at www.sciencedirect.com
ScienceDirect
Atmospheric Environment 42 (2008) 3166–3178
ATMOSPHERIC ENVIRONMENT
www.elsevier.com/locate/atmosenv

Modeling urban and regional aerosols—Development of the UCD Aerosol Module and implementation in CMAQ model

K. Max Zhang[a,*], Anthony S. Wexler[b,c,d]

[a]Sibley School of Mechanical and Aerospace Engineering, Cornell University, Ithaca, NY 14853, USA
[b]Department of Mechanical and Aeronautical Engineering, University of California, Davis, CA 95616, USA
[c]Department of Civil and Environmental Engineering, University of California, Davis, CA 95616, USA
[d]Department of Land, Air, and Water Resources, University of California, Davis, CA 95616, USA

Received 13 July 2007; received in revised form 18 December 2007; accepted 18 December 2007

Abstract

This paper presents a mechanistic, fully dynamic, internally mixed, sectional aerosol module, the UCD Aerosol Module, which evolves from the Aerosol Inorganic Model (AIM). The UCD Aerosol Module employs three gas-to-particle mass transport schemes, replacement, coupled and uncoupled, and simplified aerosol thermodynamics to predict gas–particle partitioning, aerosol phase state and water content efficiently and reasonably. Aerosol dynamics is integrated using an Asynchronous Time-Stepping (ATS) integration method, where different sized particles integrate with different time scales. CMAQ-UCD is an implementation of the UCD Aerosol Module in the CMAQ modeling system. With all of these features, CMAQ-UCD is designed to be a computationally efficient and scientifically sound air quality model that predicts particulate mass concentrations and size distributions over urban or regional scales for regulatory and scientific purposes.

Keywords: Air quality; Thermodynamics; Particulate matter; Aerosols; Size distribution; PM2.5

1. Introduction

Particulate matter (PM), from both anthropogenic and biological origins, poses one of the most daunting challenges to our understandings of human health, urban and regional air quality and global climate change. PM, a criteria pollutant, is regulated by the National Ambient Air Quality Standards (NAAQS). The physiological mechanisms linking PM to human health effects are currently under vigorous scientific inquiry (NAS, 2004). Its wide size range, myriad sources and complex atmospheric processes impede efforts to develop effective PM emissions control strategies. Globally, limited understanding of the mostly negative forcing associated with anthropogenic PM contributes to the greatest uncertainties in the Earth's radiation budget evaluation (Anderson et al., 2003).

Aerosol modules, simulating the transport and transformation of PM, are essential tools for advancing our knowledge of those critical environmental issues. Over the years, many aerosol modules have been

*Corresponding author. Tel.: +1 607 254 5402; fax: +1 607 255 1222.
E-mail address: kz33@cornell.edu (K.M. Zhang).

1352-2310/$ - see front matter © 2008 Elsevier Ltd. All rights reserved.
doi:10.1016/j.atmosenv.2007.12.052

developed, which differ in various aspects. Here, a brief summary is given of the major types of the aerosol modules based on their different characteristics.

1.1. Equilibrium and dynamic

Based on the treatment of gas–particle partitioning, there are equilibrium modules and dynamic modules. The aerosol modules assuming gas–particle equilibrium when partitioning volatile compounds between the vapor and condensed phases are called equilibrium models (Pilinis and Seinfeld, 1988; Nenes et al., 1998), whereas the models employing an explicit treatment of the mass transport are entitled dynamic models (Wexler et al., 1994; Sun and Wexler, 1998a, b; Jacobson, 1997). Recently, a hybrid method was developed that utilizes equilibrium assumptions for the fine aerosol mode (particles with diameters $<1\,\mu m$) and the dynamic approach for the coarse aerosol mode (Capaldo et al., 2000; Zhang et al., 2004).

1.2. Sectional (fixed-bin and moving-section methods) and modal

The particle size distribution may be represented by sectional approaches, where particle size distribution is represented by a set of discrete bins (Gelbard et al., 1980; Eldering and Cass, 1996; Jacobson, 1997; Sun and Wexler, 1998b; Morris et al., 2003; Zhang et al., 2004), and modal approaches by a superposition of lognormal modes (Binkowski and Shankar, 1995; Binkowski and Roselle, 2003).

Within the sectional framework, there are some variations. One type of formulation fixes particle section boundaries, i.e., the fixed-bin method, and the other adopts sections with moving centers or edges, i.e., the moving section method. These two methods have their advantages and disadvantages. The former needs to solve an additional condensation/evaporation term, namely the shift term (to be introduced in Eq. (1)), but is straightforward in simulating atmospheric transport between neighboring grid cells, where particles from different spatial grid cells are mix. The latter does not have the shift term, but needs to rearrange particle sections semi-empirically before atmospheric transport.

1.3. Internally mixed and source oriented

Based on representation of particulate compositions, there are internally mixed and source-oriented approaches. An internal mixture assumes that all particles of a given size have the same composition, while source-oriented approaches retain the primary particle composition so particles of the same size can have different chemical compositions (Kleeman et al., 1997).

Here, we present the UCD Aerosol Module, a mechanistic, fully dynamic, internally mixed, sectional aerosol module. We incorporate it into the Models-3/CMAQ platform (Dennis et al., 1996) and the new combined model is known as the Community Multiscale Air Quality Model with UC-Davis Aerosol Module (CMAQ-UCD). Here, we use "module" to denote a standalone operator implementation within a photochemical model, which usually contains a complete set of operators. The same module can be incorporated into different models. For example, a previous incarnation of the UCD Aerosol Module has been incorporated into the Urban Airshed Model (Sun and Wexler, 1998b).

The UCD Aerosol Module evolves from the Aerosol Inorganic Model (AIM). AIM was originally developed to simulate both aerosol thermodynamics and transport between the gaseous and particulate phases (Wexler and Seinfeld, 1990, 1991). Wexler et al. (1994) identified and analyzed the physical and chemical processes that may influence the particulate size and composition in the internally mixed aerosol dynamic equation (IMADE), and estimated their relative importance. Potukuchi and Wexler (1995a, b) moved the thermodynamic portion of AIM forward by identifying solid–aqueous phase transitions in atmospheric aerosols in both acid-neutral and acidic solutions. Sun and Wexler (1998a, b) proposed coupled transport to simulate condensation/evaporation near-acid neutrality and applied it to the 24–25 June SCAQS episode. Now AIM has been transformed into a phase equilibrium model of inorganic aerosol systems and available online at http://mae.ucdavis.edu/wexler/aim/ (Clegg et al., 1998; Wexler and Clegg, 2002). While the goal of the current AIM model is to be a flexible, highly accurate, phase equilibrium model for inorganic aerosols, CMAQ-UCD is designed to be a computationally efficient and scientifically sound air quality model for predicting particulate mass concentrations and size distributions in large urban or regional scales for regulatory and scientific purposes.

Since the mass transport of volatile species between gas and aerosol phases is governed by both a thermodynamic driving force and the transport moment of the particle size distribution (Wexler and

Potukuchi, 1998; Zhang and Wexler, 2006), we first introduce the UCD Aerosol Module by discussing those two major aspects, namely, gas–particle transport and aerosol thermodynamics, respectively. Then we explain how the integration for aerosol dynamics is accomplished using an Asynchronous Time-Stepping (ATS) integrator. Finally, we describe the incorporation of the UCD Aerosol Module into the USEPA Models-3/CMAQ system.

This is part one of a two-part series devoted to the description and testing of the aerosol module in CMAQ-UCD. In the accompanying paper (Nolte et al., 2008), we present the simulation results from the May 2002 Bay Regional Atmospheric Chemistry Experiment (BRACE).

2. Dynamic gas–particle partitioning in the UCD Aerosol Module

That a major portion of atmospheric aerosol mass is secondary in nature is indicative of the importance of gas-to-particle conversion (Hughes et al., 1999; Magliano et al., 1999). Mass transport by condensation of vapor on particles provides a major pathway for secondary PM formation. Thus, condensation and its reversal, evaporation, are essential parts of aerosol dynamics.

The equation governing condensation/evaporation in a fixed size bin formulation is (Wexler et al., 1994)

$$\frac{\partial p_i(\mu,\mathbf{x},t)}{\partial t} = \overbrace{H_i(\mu,\mathbf{x},t)p(\mu,\mathbf{x},t)}^{\text{growth}} - \overbrace{\frac{1}{3}\frac{\partial H p_i(\mu,\mathbf{x},t)}{\partial \mu}}^{\text{shift}} \quad (1)$$

In Eq. (1), $\mu = \ln(D_p)$, where D_p is particle diameter; $p_i(\mu,\mathbf{x},t)\,d\mu$ is the mass concentration of species i between μ and $\mu + d\mu$ at location x and time t, and $p = \sum_{i=1}^{s} p_i$; $H_i = (dm_i/dt)/m$ is the normalized condensation rate of species i and $H = \sum_{i=1}^{s} H_i$, where m_i is the mass of species i in an individual particle of total mass $m = \sum_{i=1}^{s} m_i$. The first term on the right hand side of Eq. (1) acts as the *growth* term because it moves the distribution higher or lower in response to condensation or evaporation, respectively, while the second term *shifts* the distribution to larger or smaller particle sizes in response to condensation or evaporation, respectively.

Here, we first review two condensation/evaporation schemes developed earlier, i.e., uncoupled and coupled mass transport, and then introduce a new scheme, namely, replacement mass transport. This section is concluded by a description on how these three schemes are implemented in the UCD Aerosol Module.

2.1. Uncoupled transport

Conventionally, gas–particle transport is modeled as *uncoupled* by Eq. (2), where "uncoupled" means that species transport rates are independent of each other (Wexler et al., 1994):

$$H_i = Mw_i \frac{2\pi D_p D_i}{m} \frac{c_i - c_{i,\text{surf}}}{1+\gamma} \quad \text{(uncoupled transport)} \quad (2)$$

In Eq. (2), c_i, and $c_{i,\text{surf}}$ are the mole concentrations of species i in the gas phase and over the particle surface, respectively; D_i and Mw_i are the diffusivity and molecular weight of species i, respectively; the factor γ accounts for the non-continuum effects and the imperfect accommodation of the condensate on the particle surface, the latter of which is described by the accommodation coefficient, α_i. For most purposes, a sufficient approximation is $\gamma \approx 8\lambda/\alpha_i D_p$ (Wexler and Seinfeld, 1990; Bowman et al., 1997), where λ is the air mean free path (around 0.065 μm at 298 K).

2.2. Coupled transport

Coupled transport, Eq. (3), where acid and base condense or evaporate together, was first proposed by Wexler and Seinfeld (1990) for condensation of ammonia and volatile acid to form the solid crystalline salt form and then used by Sun and Wexler (1998a) for acid-neutral condensation/evaporation simulations (Sun and Wexler, 1998b; Capaldo et al., 2000; Pilinis et al., 2000):

$$H_i = Mw_i \frac{\pi D_p \bar{D}\bar{c}(1+\gamma)}{m} \times \left[1 - \sqrt{1 - 4\frac{c_{NH_3,\infty}c_{HX,\infty} - K_{NH_3X}}{\bar{c}^2(1+\gamma)^2}}\right] \quad \text{(coupled transport)} \quad (3)$$

where $\bar{D} = \sqrt{D_{NH_3} D_{HX}}$ is the average diffusivity; $\bar{c} = (D_{NH_3} c_{NH_3,\infty} + D_{HX} c_{HX,\infty})/\bar{D}$ is the diffusion weighted average of the concentrations far from the particle; $c_{NH_3,\infty}$ and $c_{HX,\infty}$ are the ambient concentrations of ammonia and a volatile acid; and K_{NH_3X} is the partial pressure product at the surface of the particle, i.e., $c_{NH_3,\text{surf}} \times c_{HX,\text{surf}}$.

Since ammonia is the most important basic volatile species in the atmosphere, its existence in gas or particle phase is required for a coupled transport. One of the most important advantages of coupled transport is its pH independence. Hydrogen ion is one of the modeled species in most aerosol models and determines the particle pH. The vapor pressures of volatile species are very sensitive to pH. However, pH changes abruptly in response to a small amount of condensation or evaporation of an acid–base species; even small numerical error such as numerical diffusion in an advection solver could cause errors in hydrogen ion concentration, leading to a sharp change in pH value. All these make condensation/evaporation difficult to integrate (Sun and Wexler, 1998a). With coupled transport, the terms depending on pH cancel each other in the vapor pressure product, K_{NH_3X}, thus reducing the stiffness in the aerosol dynamics system under near-acid-neutral conditions (Zhang and Wexler, 2006).

2.3. Replacement transport

In the absence of ammonia, another possibility for acid-neutral condensation/evaporation is the reversible displacement reaction that may occur where condensation of nitric acid causes hydrochloric acid to evaporate, or vice versa. Next, we will derive the equation for this type of transport, termed replacement transport, and demonstrate its pH independence. Sulfuric acid condensation will also displace volatile acids from particle phase, but sulfuric acid is regarded as nonvolatile, which makes the displacement process much easier to simulate.

Suppose that we have a displacement reaction:

$$HX_i(g) + HX_j(aq) \leftrightarrow HX_i(aq) + HX_j(g) \qquad (R1)$$

where HX_i and HX_j can be either HCl or HNO_3. The continuity equations for HX_i and HX_j can been written as

$$\frac{D_i}{r^2}\frac{d}{dr}\left(r^2\frac{dc_i}{dr}\right) = \frac{D_j}{r^2}\frac{d}{dr}\left(r^2\frac{dc_j}{dr}\right) = 0 \qquad (4)$$

where c_i and c_j are the molar gas-phase concentrations, and D_i and D_j are the molecular diffusivities for HX_i and HX_j, respectively (Wexler and Seinfeld, 1990). The boundary conditions for this differential equation are (a) far from the particle and gas-phase concentrations of HX_i and HX_j are known:

$$c_i(r \to \infty) = c_{i,\infty}$$

$$c_j(r \to \infty) = c_{j,\infty}$$

and (b) at the particle surface, the influx of HX_i must balance the efflux of HX_j according to (R1) so the boundary conditions are

$$D_i\left.\frac{dc_i}{dr}\right|_{r=R_p} = -D_j\left.\frac{dc_j}{dr}\right|_{r=R_p} = \alpha k_{coll}(c_{i,R_p}c_{j,surf} - c_{i,surf}c_{j,R_p})$$

where R_p is the particle radius and k_{coll} is the collision-limited surface reaction rate constant and α is the accommodation coefficient.

The concentration profiles of HX_i and HX_j that satisfy the differential equations and the boundary conditions at infinity are

$$c_i(r) = A_i\frac{R_p}{r} + c_{i,\infty} \quad \text{and} \quad c_j(r) = A_j\frac{R_p}{r} + c_{j,\infty} \qquad (5)$$

where the A_i and A_j are arbitrary constants (Wexler and Seinfeld, 1990). Applying the second boundary conditions at the particle surface gives:

$$J_i = -J_j = \frac{4\pi R_p^2\alpha k_{coll}(c_{i,\infty}c_{j,surf} - c_{i,surf}c_{j,\infty})}{1 + (\alpha k_{coll}R_p/D_j)c_{i,surf} + (\alpha k_{coll}R_p/D_i)c_{j,surf}} \qquad (6)$$

Assuming $D_i = D_j = D$:

$$J_i = -J_j = \frac{4\pi R_p D}{1+\gamma}\left(\frac{c_{i,\infty}c_{j,surf} - c_{j,\infty}c_{i,surf}}{c_{i,surf} + c_{j,surf}}\right) \qquad (7)$$

where $\gamma = D/(\alpha R_p k_{coll}(c_{i,surf} + c_{j,surf}))$ can be approximated by $8\lambda/\alpha D_p$.

The corresponding H_i in Eq. (1) can be estimated from mass flux to a single particle which gives

$$H_i = Mw_i\frac{1}{m}\frac{2\pi D_p D}{1+\gamma}\left(\frac{c_{i,\infty}c_{j,surf} - c_{j,\infty}c_{i,surf}}{c_{i,surf} + c_{j,surf}}\right) \quad \text{(replacement)} \qquad (8)$$

The only possible pH dependence in Eq. (8) is $c_{j,surf}/c_{i,surf}$, but both $c_{j,surf}$ and $c_{i,surf}$ are proportional to $[H^+]$, so the dependence cancels.

Although we proposed replacement transport in the absence of ammonia, it can also be important in presence of ammonia. In fact, coupled transport of both NH_4NO_3 and NH_4Cl already encompasses replacement transport. Let us consider the coupled transports of two volatile acids in reverse

directions

$$HNO_3(g) + NH_3(g) \leftrightarrow NH_4(aq) + NO_3^-(aq)$$
$$\text{or} \quad HNO_3(g) + NH_3(g) \leftrightarrow NH_4NO_3(s) \qquad \text{(R2)}$$

$$NH_4(aq) + Cl^-(aq) \leftrightarrow HCl(g) + NH_3(g)$$
$$\text{or} \quad NH_4Cl(s) \leftrightarrow HCl(g) + NH_3(g) \qquad \text{(R3)}$$

Combining (R2) and (R3) gives

$$HNO_3(g) + Cl^-(aq) \leftrightarrow HCl(g) + NO_3^-(aq)$$
$$\text{or} \quad HNO_3(g) + NH_4Cl(s) \leftrightarrow HCl(g) + NH_4NO_3(s) \qquad \text{(R4)}$$

(R4) is the replacement reaction (R1) we discussed previously.

2.4. Applications of transport mechanisms

So far we have introduced three main transport mechanisms used in the UCD Aerosol Module, i.e., coupled transport, uncoupled transport and replacement transport, with expressions given in Eqs. (2), (3) and (8), respectively, but we need to clarify under what conditions these mechanisms should be employed. Generally speaking, coupled and replacement transport can only be applied under near-acid neutrality conditions and the uncoupled transport is to be used otherwise.

In the UCD Aerosol Module, we first determine whether the near-acid neutrality condition is met. If not, the uncoupled transport is used. Otherwise, the scheme presented in Table 1 is utilized. Since the intrinsic properties of all three transport mechanisms enable them to automatically determine the direction of gas–particle transfer, i.e., condensation or evaporation, the abundance or scarcity of the total concentrations of volatile species in both gas and particle phase, as represented by T_A, T_N and T_C in Table 1, become the most critical factors determining which mechanism(s) to use. First, if the total concentrations of all three volatile species are small (Case 1), the aerosol dynamics calculation is skipped. This is often the case when the model is simulating a large domain, where many cells may contain an insignificant amount of pollutants and skipping aerosol dynamics will have negligible effect on modeling results. Next, if only one out of three volatile species is in significant concentrations while the other two are not (Cases 2, 3 and 4), uncoupled transport is invoked. If we have abundant T_A, and T_N, or T_A and T_C (Cases 5 and 6), coupled transport is used for that acid–base combination. But if the abundant species are HNO_3 and HCl (Case 7), the replacement transport is chosen. Finally, if all three volatile species are abundant (Case 8), we simulate the coupled transport of both acid–base combinations, NH_4NO_3 and NH_4Cl. Double coupled transport can simulate replacement, if appropriate, by one pair condensing and the other evaporating.

Table 1
Application of replacement, coupled and uncoupled transport mechanisms

Case ID	T_A	T_N	T_C	Mechanism(s) used
1				No aerosol thermodynamics
2	X			Uncoupled
3		X		Uncoupled
4			X	Uncoupled
5	X	X		Coupled NH_3 and HNO_3
6	X		X	Coupled NH_3 and HCl
7		X	X	Replacement
8	X	X	X	Coupled NH_3 and HNO_3, NH_3 and HCl

T_A: total ammonia, T_N: total nitrate, T_C: total chloride. X denotes that T_i exceeds the user-defined threshold value for species i.

3. Particle thermodynamics

As we mentioned previously, mass transport of a volatile compound between gas and particle phases, also known as gas–particle partitioning, is driven by the differences between partial pressure far from particles, equivalent to its ambient concentration, and its equilibrium vapor pressure at the particle surface. The thermodynamic portion of aerosol modules determines: (1) the equilibrium vapor pressures of volatile species given aerosol composition, temperature and relative humidity; and (2) water content associated with the particulate composition. AIM calculates the equilibrium state using Gibbs free energy minimization, which is sufficiently fast for analysis of experimental data, but too slow to be incorporated into large-scale atmospheric models. The detailed phase state information, while useful for other purposes, may not be necessary for gas–particle partitioning. In addition, metastable states may cause departures from thermodynamic equilibrium, but the existence of these states depends on many factors including the history of the particles' phase state, which is computationally intractable—thermodynamic

equilibrium is assumed here, as in most atmospheric aerosol models. Motivated by this objective, the UCD Aerosol Module employs a simplified thermodynamics model of the H^+–NH_4^+–Na^+–SO_4^{2-}–NO_3^-–Cl^- system, with HNO_3, HCl and NH_3 being the volatile compounds and NH_4NO_3 and NH_4Cl as two volatile salts. H_2SO_4 is treated as a volatile compound with effective equilibrium vapor pressure as zero. This thermodynamic model, without Gibbs free energy minimization, is considerably faster than, but not as accurate as, AIM. The major components of aerosol thermodynamics, such as equilibrium reactions and constants, are inherited from early modeling efforts (Potukuchi and Wexler, 1995a, b). So we only report the recent development in this section and readers are referred to those early publications for detailed descriptions.

3.1. Existence of solid-phase ammonium salts

In a polluted urban environment, the ammonium salts usually account for a significant fraction of the fine aerosol mass (Heintzenberg, 1989; Hughes et al., 1999). Furthermore, the only two volatile solids in the typical aerosol thermodynamics system mentioned earlier are ammonium salts, i.e., ammonium nitrate and ammonium chloride. So it is an important task to accurately simulate their thermodynamics in the atmosphere. In the UCD Aerosol Module, a simple and accurate method was adopted to predict the phase state of ammonium salts.

Consider the vapor–aqueous equilibrium reaction of ammonium nitrate (R2), which can be similarly applied to ammonium chloride:

$$NH_4^+(aq) + NO_3^-(aq) \leftrightarrow NH_3(g) + HNO_3(g)$$

Based on the equilibrium equation, we have $p_{NH_3} \times p_{HNO_3} = K_{AN}\gamma_{AN}^2 m_{AN}^2$, where p_{NH_3} and p_{HNO_3} are the equilibrium vapor pressures of NH_3 and HNO_3 over the particle surface, respectively; γ_{AN} and m_{AN} represent the activity coefficients and molalities of ammonium nitrate, respectively ($\gamma_{AN}^2 = \gamma_{NH_4^+}\gamma_{NO_3^-}$ and $m_{AN}^2 = m_{NH_4^+} m_{NO_3^-}$); K_{AN} is the equilibrium constant for the reaction.

For the solid–vapor equilibrium for ammonia and nitric acid, reaction (R2) is

$$NH_4NO_3(s) \leftrightarrow NH_3(g) + HNO_3(g)$$

Since the activity of solid ammonium nitrate is 1, we have $p_{NH_3} \times p_{HNO_3} = K_{AN}$, so that at a given temperature, the presence of ammonium nitrate solid sets the upper limit for the partial pressure product of ammonia and nitric acid vapors (Wexler and Potukuchi, 1998). The solid–vapor pressure product and the non-ideal NH_4NO_3 solution curve join at saturation, which has been shown in previous studies (Stelson and Seinfeld, 1982). Here, we demonstrate this relationship under different temperatures using the UCD Aerosol Module for ammonium nitrate in Fig. 1. Comparison against the results obtained from the more accurate AIM model shows that the simplified aerosol thermodynamics adopted in the UCD Aerosol Module largely reproduces the deliquescence relationship and temperature dependence from AIM. However, as shown in Fig. 1, the UCD Aerosol Module tends to somewhat over-predict the vapor pressure for low temperatures.

In practice, we calculate the partial pressure product assuming a pure aqueous solution. If the value of the product is larger than K_{AX}, i.e., K_{AN} or K_{AC}, the existence of solid phase salts is identified and the product is kept constant as K_{AX}. The related equilibrium parameters are reported in Table 2.

3.2. Deliquescence, MDRH and phase states

There are three possible phase states for a given particulate composition, relative humidity and temperature, i.e., pure aqueous, pure solid and aqueous–solid mixture. These different states are closely related to the deliquescence behavior of aerosols. The deliquescence point for multiple-salt solutions, the so-called mutual deliquescence relative humidity (MDRH), is lower than that of single-salt solutions and only dependent on particulate composition and temperature (Wexler and Seinfeld, 1991). In the UCD Aerosol Module, we first approximate combination of solids that may exist at the correct temperature and look up the MDRH for that composition (the procedure will be explained later). The aerosol phase is assumed to be in pure solid state when the RH is below the MDRH. If RH is higher than MDRH, the RH is compared with the deliquescence relative humidity (DRH) of each salt available in the solid mixture. If the RH is higher than the DRH of any possible salts, the particle phase is assumed to be pure aqueous. Otherwise, it is an aqueous–solid mixture. If this is the case, the salt whose DRH exceeds RH is recorded and that DRH is set to RH_{wet} as suggested in ISORROPIA (Nenes et al., 1998). If the DRH of two or more salts exceeds RH, the lowest DRH is set to RH_{wet}. RH_{wet} characterizes how far the

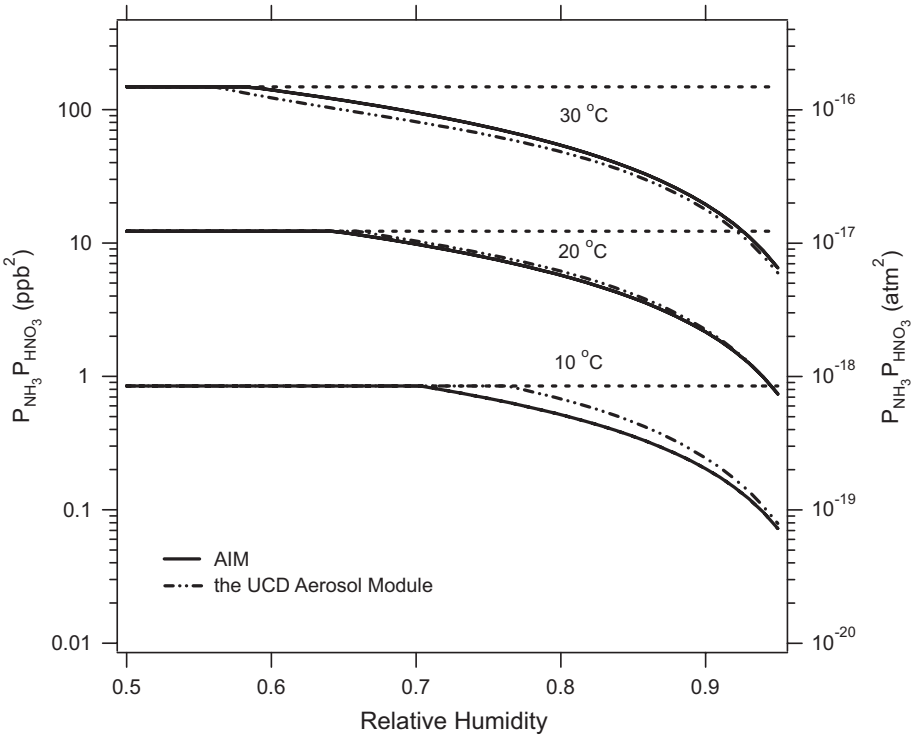

Fig. 1. Vapor pressure product of NH_3 and HNO_3 in saturation and non-ideal solutions at different temperature simulated by AIM (solid lines) and the UCD Aerosol Module (dotted lines). At a given temperature, the presence of ammonium nitrate solid sets the upper limit for the partial pressure product of ammonia and nitric acid vapors.

Table 2
Equilibrium parameters for solid–vapor equilibrium of ammonium salts

Reaction	Constant expression	K_{AX} (atm^2) at 298.15 K	$\Delta H^\circ/RT_0$	$\Delta C_p^\circ/R$
$NH_4NO_3(s) = NH_3(g) + HNO_3(g)$	$K_{AN} = p_{NH_3} \times p_{HNO_3}$	4.356×10^{-17}	74.32	−1.24
$NH_4Cl(s) = NH_3(g) + HCl(g)$	$K_{AC} = p_{NH_3} \times p_{HNO_3}$	7.985×10^{-17}	71.10	−2.40[a]

The values are obtained from AIM model (Clegg et al., 1998; Wexler and Clegg, 2002) except otherwise noted.
[a]From Wagman et al. (1982).

aerosol system is from deliquescence and is used to determine particle water content.

In the UCD Aerosol Module, a semi-empirical method was adopted to determine MDRH. First, we examine whether the solution contains a deliquescent salt mixed with a non-deliquescent electrolyte such as sulfuric acid. If so, MDRH is equal to zero. This is called the free acid region, parameterized by $[H^+]/[SO_4^{2-}] > 1$.

Next, we approximate the possible solid composition in non-free acid conditions. In this H^+–NH_4^+–Na^+–SO_4^{2-}–NO_3^-–Cl^- system, we consider 15 possible solid forms, $Na_2SO_4 \cdot (NH_4)_2SO_4 \cdot 4H_2O$, $NaNO_3 \cdot Na_2SO_4 \cdot H_2O$, $Na_3H(SO_4)_2$, $(NH_4)_3H(SO_4)_2$, $3NH_4NO_3 \cdot (NH_4)_2SO_4$, $2NH_4NO_3 \cdot (NH_4)_2SO_4$, Na_2SO_4, $NaHSO_4$, $(NH_4)_2SO_4$, NH_4HSO_4, NaCl, $NaNO_3$, NH_4Cl, NH_4NO_3. The algorithm (1) forms single salts, and combined them to make double salts; (2) forms the salts with higher DRH before those with lower DRH. The reasoning here is that salts with higher DRH usually occupy larger phase space as demonstrated in previous studies (Wexler and Seinfeld, 1991; Potukuchi and Wexler, 1995a, b).

The process starts with chlorides, since chlorides only have two simple forms, NaCl and NH_4Cl. We let NH_4Cl form first, so the remaining chloride is associated with sodium. When no free acids exist, hydrogen ion has to be associated with sulfate anion to form either bisulfate or $H(SO_4)_2^{3-}$. When $0.5 < [H^+]/[SO_4^{2-}] < 1$, we have the mixture of HSO_4^-

and $H(SO_4)_2^{3-}$. The ratio of HSO_4^- over $H(SO_4)_2^{3-}$ can be simply derived from mass balance of hydrogen and sulfate. When $[H^+]/[SO_4^{2-}]<0.5$, all hydrogen exists as $H(SO_4)_2^{3-}$. Next, we let $(NH_4)_3H(SO_4)_2$ form before $Na_3H(SO_4)_2$, and NH_4HSO_4 before $NaHSO_4$. Similarly, we let Na_2SO_4 form before $(NH_4)_2SO_4$ to finish the sulfates, and $NaNO_3$ before NH_4NO_3 to finish the nitrates. This completes single salt formation. The sequence for the double salts formation is $Na_2SO_4\cdot(NH_4)_2SO_4\cdot 4H_2O$ first, $NaNO_3\cdot Na_2SO_4\cdot H_2O$ second and nitrate double salts last.

We ran the AIM model (http://mae.ucdavis.edu/wexler/aim/) to predict the MDRH for different solid compositions, and found the characteristic salts, which govern MDRH values for different relative compositions of the same ionic system, are usually the salts with the lowest DRH. The AIM model results are listed in Table 3. Thus, once the solid composition is determined, the characteristic salt in that composition is determined and the MDRH is read from values in Table 3. This semi-empirical method predicts MDRH values for most ionic systems in good agreement with AIM.

3.3. Water content

The water content associated with aerosol salts are calculated using ZSR (Stokes and Robinson, 1966). In our early modeling, the single solute molality values were acquired by a series of polynomials (Potukuchi and Wexler, 1995a). In the UCD Aerosol Module, we apply single solute molality data compiled from numerous experiments by Clegg et al. (1998) for the AIM model, and interpolate for the appropriate RH and temperature.

Here, we used the same approach as in ISSORROPIA (Nenes et al., 1998) to determine particle water content in a mixed phase state. The particle composition is a weighted mean of two states, one in which there is no water ("dry" state) and one in which the most hygroscopic salt (i.e., with the lowest DRH) is completely dissolved ("wet" state). The weighting factor, c, is defined as

$$c=\frac{\mathrm{MDRH}-\mathrm{RH}}{\mathrm{MDRH}-\mathrm{RH_{wet}}} \quad (9)$$

Aerosol water content is proportional to the weighting factor, and specifically is equal to $c\cdot(H_2O)_{wet}$, where $(H_2O)_{wet}$ is the water content of the "wet" solution (Nenes et al., 1998).

Table 3
Characteristic salts in various ionic systems to determine MDRH

Ionic system	Characteristic salts	MDRH
NH_4^+, SO_4^{2-}, NO_3^-	NH_4NO_3	0.601
	$3NH_4NO_3\cdot(NH_4)2SO_4$	0.635
	$2NH_4NO_3\cdot(NH_4)2SO_4$	0.655
NH_4^+, SO_4^{2-}, Cl^-[a]		0.720
NH_4^+, NO_3^-, Cl^-[a]		0.546
Na^+, SO_4^{2-}, NO_3^-	$NaNO_3$	0.734
	$NaNO_3\cdot Na_2SO_4\cdot H_2O$	0.806
Na^+, SO_4^{2-}, Cl^-[a]		0.743
Na^+, NO_3^-, Cl^-[a]		0.672
NH_4^+, Na^+, SO_4^{2-}	$(NH_4)2SO_4$	0.770
	$Na_2SO_4\cdot(NH_4)2SO_4\cdot 4H_2O$	0.822
NH_4^+, Na^+, NO_3^-[a]		0.500
NH_4^+, Na^+, Cl^-[a]		0.692
H^+, NH_4^+, SO_4^{2-}	NH_4HSO_4	0.367
	$(NH_4)3H(SO_4)_2$	0.688
H^+, NH_4^+, SO_4^{2-}	$NaHSO_4$	0.534
	$Na_3H(SO_4)_2$	0.698
NH_4^+, SO_4^{2-}, NO_3^-, Cl^-	NH_4NO_3	0.538
	$3NH_4NO_3\cdot(NH_4)2SO_4$	0.568
	$2NH_4NO_3\cdot(NH_4)2SO_4$	0.587
Na^+, SO_4^{2-}, NO_3^-, Cl^-	$NaNO_3$	0.669
	NaCl	0.704
H^+, NH_4^+, Na^+, SO_4^{2-}[b]	NH_4HSO_4	0.330
	$Na_3H(SO_4)_2$	0.545
	Na_2SO_4	0.553
	$Na_2SO_4\cdot(NH_4)2SO_4\cdot 4H_2O$	0.653
NH_4^+, Na_4^+, SO_4^{2-}, NO_3^-	NH_4NO_3	0.484
	$3NH_4NO_3\cdot(NH_4)2SO_4$	0.515
	$2NH_4NO_3\cdot(NH_4)2SO_4$	0.604
	$NaNO_3\cdot Na_2SO_4\cdot H_2O$	0.679
NH_4^+, Na^+, SO_4^{2-}, Cl^-[b]	NaCl	0.676
	Na_2SO_4	0.683
	$(NH_4)2SO_4$	0.693
NH_4^+, Na^+, NO_3^-, Cl^-	NH_4NO_3	0.440
	$NaNO_3$	0.544
H^+, NH_4^+, SO_4^{2-}, NO_3^-	$NH_4NO_3\cdot NH_4HSO_4$	0.320
	NH_4NO_3	0.486
	$3NH_4NO_3\cdot(NH_4)2SO_4$	0.543
	$2NH_4NO_3\cdot(NH_4)2SO_4$	0.573
H^+, NH_4^+, SO_4^{2-}, Cl^-	NH_4HSO_4	0.360
	$(NH_4)3H(SO_4)_2$	0.648
H^+, Na^+, SO_4^{2-}, NO_3^-[b]	$NaHSO_4$	0.452
	$NaNO_3$	0.594
	Na_2SO_4	0.661
H^+, Na^+, SO_4^{2-}, Cl^-	$NaHSO_4$	0.511
	$Na_3H(SO_4)_2$	0.661

Table 3 (*continued*)

Ionic system	Characteristic salts	MDRH
NH_4^+, Na^+, SO_4^{2-}, NO_3^-, Cl^-	NH_4NO_3	0.429
	$3NH_4NO_3 \cdot (NH_4)2SO_4$	0.480
	$2NH_4NO_3 \cdot (NH_4)2SO_4$	0.533
	$NaNO_3$	0.538
	$NaNO_3 \cdot Na_2SO_4 \cdot H_2O$	0.590
H^+, Na^+, SO_4^{2-}, NO_3^-, Cl^-	$NaHSO_4 \cdot H_2O$	0.440
	$NaNO_3$[b]	0.576
	$NaNO_3 \cdot Na_2SO_4$[b]	0.627
H^+, NH_4^+, SO_4^{2-}, NO_3^-, Cl^-	$NH4NO_3 \cdot NH_4HSO_4$	0.305
	NH_4NO_3	0.455
	$3NH_4NO_3 \cdot (NH_4)2SO_4$	0.508

[a]Denote the ionic system has only one MDRH point.
[b]Denotes the characteristic salt is not the salt with the lowest DRH.

4. Integration scheme

While the numerical scheme for solving the "shift" term has been reported earlier (Dhaniyala and Wexler, 1996), the numerical integration for the "growth" term in Eq. (1) is accomplished by the ATS integrator (Zhang and Wexler, 2006).

The implementation of ATS in the UCD Aerosol Module is shown in Fig. 2. Each size section j has its own integration time, denoted as t^j and calculated by considering the timescales for species in both the gaseous and particulate phases. There are also the current global time t_{curr} and updated global time t_{new}. At the start of the integration, each t^j is set to t_{curr}. The aerosol water content is updated in accordance with the particle composition and ambient relative humidity. The condensation rates of species i in size bin j, H_i^j, and integration time step for each size section Δt^j are calculated. The new global time t_{new} is determined by updating t_{curr} by the longest Δt^j.

Then, integration is carried out for each size section according to its own integration time step for each volatile or condensable species (in Fig. 2, this is denoted as "grow C_i^j"). A sorting algorithm implements dynamic timescale ordering, i.e., the sections with smaller timescales are integrated before those with larger timescales. After each integration, the ambient gas species concentration and particle water content are updated ("update gases" and "fix water"). The condensation rate for water H_w^j and the total condensation rate for this size section, $\bar{H}^j$, which will be used later in the calculation of the "shift" in size coordinate, are now calculated. The time for the size section t^j is then updated. Then a check is performed to determine if this size section has "caught up" with the new global time t_{new} ("$t^j > t_{new}$?"). For all size sections that have not caught up with t_{new}, another pass of integration will be performed. When all size sections have caught up to t_{new} ("complete = 0"), the current global time is updated to t_{new} and a check will determine if the mass of the size sections has changed significantly enough to warrant a shift in size coordinate will need to be calculated. If not, the program will go back to another "grow" loop. Users can choose to implement dynamic timescale ordering before a new "grow" loop. Speed and accuracy tests of ATS are reported in Zhang and Wexler (2006).

5. Incorporating the UCD Aerosol Module into the Models-3/CMAQ platform

5.1. Operator splitting in Models-3/CMAQ

The host model for CMAQ-UCD, Models-3/CMAQ developed by USEPA Atmospheric Modeling Division, is a three-dimensional Eulerian modeling system that simulates the transport, physical transformation, and chemical reactions of multiple pollutants across large geographic regions (Dennis et al., 1996; Binkowski and Roselle, 2003; Byun and Schere, 2006). The Chemical Transport Model (CTM) of Models-3/CMAQ employs operator splitting such that

$$c_i(\mathbf{x}, t + \Delta t) = L_{vdiff} L_{hadv} L_{zadv} L_{hdiff} L_{chem} L_{cloud} L_{aero} c_i(\mathbf{x}, t) \quad (10)$$

where $c_i(\mathbf{x}, t)$ is the concentration of species i and Δt is the operator time step; L_{vdiff}, L_{hadv}, L_{zadv}, L_{hdiff}, L_{chem}, L_{cloud} and L_{aero} are the operators for vertical diffusion, horizontal advection, vertical advection, horizontal diffusion, gas chemistry, cloud process and aerosol processes, respectively. Among these operators, L_{vdiff}, L_{hadv}, L_{zadv}, L_{hdiff} are, for the most parts, identical for the gaseous phase and particulate phase species in the fixed-bin sectional approach; L_{chem} is for gaseous phase species only. We first replace the original L_{aero} in the standard version of CMAQ with the UCD Aerosol Module. We have made the code interface so that it can be easily adapted to the platforms other than Models-3/CMAQ. In addition, we (1) adapt CMAQ into sectional formulation and (2) update L_{cloud}.

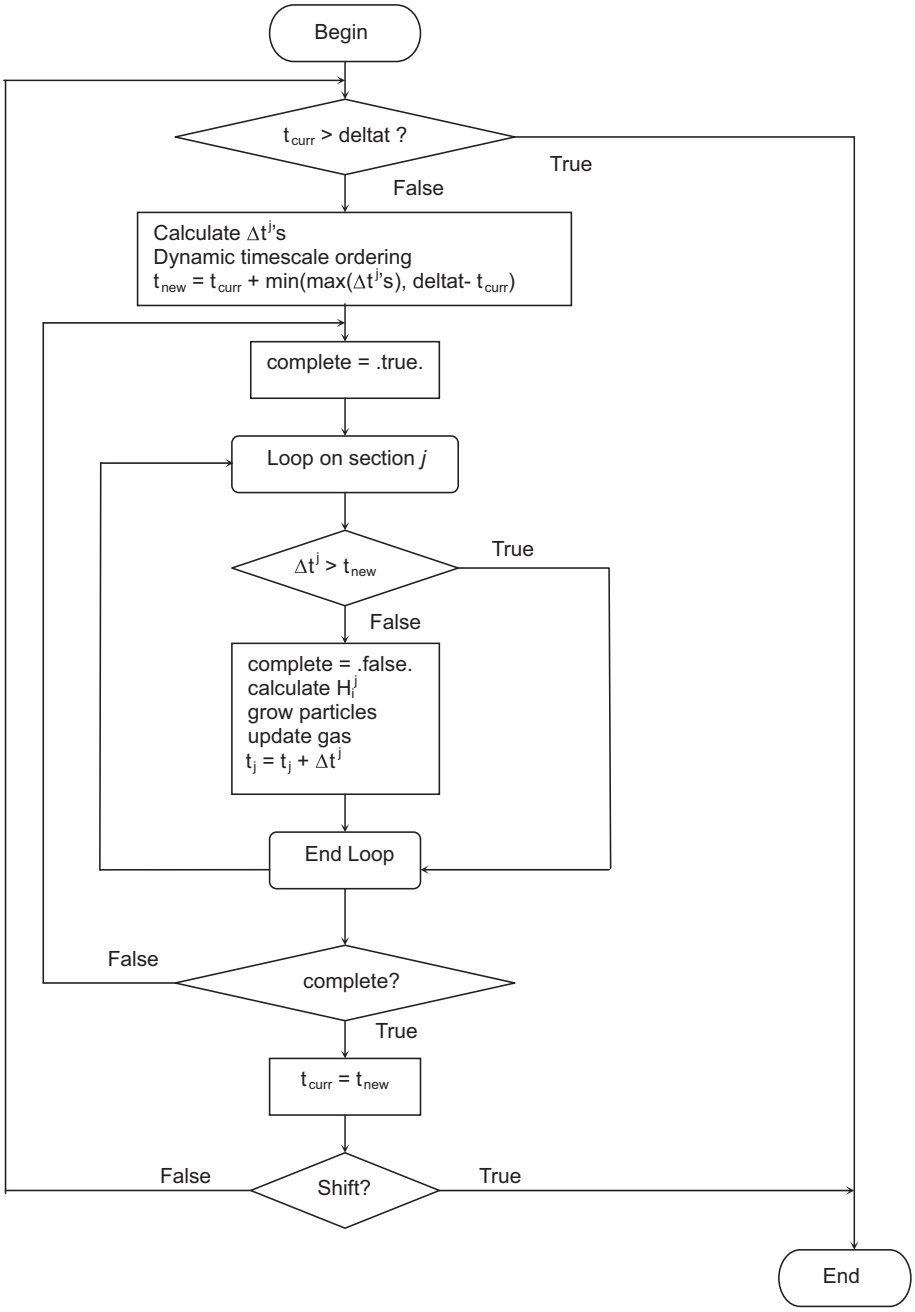

Fig. 2. ATS integration scheme diagram.

The following subsections are devoted to each of the procedures.

5.2. Adapting CMAQ to sectional formulation

One of the most distinct differences between Models-3/CMAQ and CMAQ-UCD is that the former adopt a modal approach to represent particle size distributions while the latter takes a sectional approach. For Models-3/CMAQ users, the initial and boundary conditions as well as PM emission inventories are prepared in modal forms. Thus, CMAQ-UCD has to partition these input data into sectional forms based on their lognormal parameters, i.e., mass, mean diameters and standard deviations. Currently, we take an "on-line" approach, i.e., reading the modal input data and processing them into sectional representations within the CTM. The advantages are that users do not need to take extra steps in processing the input data

and disk usage is relatively low, while the disadvantage is that the processing itself may take some CPU time. In the event that the input data are already in sectional forms, this step may be skipped.

The dry deposition code is also updated in CMAQ-UCD so that the deposition velocity is computed for each size section, consistent with rest of the model.

5.3. Cloud operator

To adapt the current cloud module in Models-3/CMAQ into a sectional formulation while maintaining its original science algorithm as much as possible, we make several assumptions. Because each activated particle is expected to grow to about the same size, the total sulfate production by heterogeneous oxidation for each size section is proportional to the number density of that section (Sun, 1999).

In a precipitating cloud, droplets will become raindrops when their sizes have grown so large that their settling velocity becomes significant. The percentage of mass reduced by wet deposition is the same for all activated size sections and all aerosol species within each size sections. Unactivated particles can also be scavenged by falling raindrops and brought to the ground, but in the present model configuration this is not considered. Hence, cloud processing aerosol mass can be increased by aqueous chemical reactions but also decreased by wet deposition.

6. Conclusion

CMAQ-UCD consists of conventional Models-3/CMAQ with the aerosol modules replaced by the UCD Aerosol Module. In addition, we update the aerosol related components in Models-3/CMAQ, especially in the initial/boundary conditions, emissions, deposition and cloud processor, to adapt them to a sectional formulation from the modal approach. Compared to the current aerosol modules in Models-3/CMAQ, the UCD Aerosol Module is sectional, fully dynamic and treats the sea-salt aerosol thermodynamics explicitly. The dynamic gas–particle mass transport is accomplished by three schemes, namely, the conventional uncoupled transport and the pH-independent coupled transport and replacement transport. The pH-independence of the last two schemes enables us to avoid the numerical stiffness typical in near-acid neutral conditions and thus improve the computational efficiency. Furthermore, several mechanisms have been developed to speed up the aerosol thermodynamics simulations in the UCD Aerosol Module. As a result of solid–aqueous phase equilibrium, the equilibrium constants of solid–vapor reactions pose an upper limit on the vapor pressure products of aqueous–vapor reactions. By taking advantage of this feature, we introduce a straightforward way to determine the existence of solid ammonium salts, the most dominant volatile salts in typical aerosol compositions. MDRH is determined by a fast and semi-empirical method. Water content is calculated based on the relative humidity, temperature and phase state characterized by the MDRH. Finally, the numerical integration of the aerosol dynamics system is mainly accomplished by the ATS integrator. ATS integrates different species based on their intrinsic timescales, reducing the stiffness of the system and number of integrations.

CMAQ-UCD is designed to be a computationally efficient and scientifically sound air quality model that predicts particulate mass concentrations and size distributions over urban or regional scales for regulatory and research purposes. In an accompanying work (Nolte et al., 2008), the CMAQ-UCD is tested on data from the BRACE field campaign.

Acknowledgments

This work was supported by US Environmental Protection Agency (USEPA) via a University Corporation for Atmospheric Research (UCAR) Fellowship and the California Air Resources Board (CARB). The authors want to thank Dr. Robin Dennis at USEPA Atmospheric Modeling Division, Dr. Ajith Kaduwela at CARB and the staff in UCAR Visiting Scientist Program for their help.

References

Anderson, T.L., Charlson, R.J., Schwartz, S.E., Knutti, R., Boucher, O., Rodhe, H., Heintzenberg, J., 2003. Climate forcing by aerosols—a hazy picture. Science 300 (5622), 1103–1104.

Binkowski, F.S., Roselle, S.J., 2003. Models-3 community multiscale air quality (CMAQ) model aerosol component—1. Model description. Journal of Geophysical Research-Atmospheres 108 (D6) (art. no. 4183).

Binkowski, F.S., Shankar, U., 1995. The regional particulate model 1. Model description and preliminary results. Journal of Geophysical Research-Atmospheres D 12 (100), 26191–26209.

Bowman, F.M., Odum, J.R., Seinfeld, J.H., Pandis, S.N., 1997. Mathematical model for gas–particle partitioning of secondary organic aerosols. Atmospheric Environment 31 (23), 3921–3931.

Byun, D., Schere, K.L., 2006. Review of the governing equations, computational algorithms, and other components of the Models-3 Community Multiscale Air Quality (CMAQ) modeling system. Applied Mechanics Reviews 59, 51–77.

Capaldo, K.P., Pilinis, C., Pandis, S.N., 2000. A computationally efficient hybrid approach for dynamic gas/aerosol transfer in air quality models. Atmospheric Environment 34 (21), 3617–3627.

Clegg, S.L., Brimblecombe, P., Wexler, A.S., 1998. A thermodynamic model of the system H-NH_4–Na–SO_4–NO_3–Cl–H_2O at 298.15 K. Journal of Physical Chemistry 102A, 2155–2171.

Dennis, R.L., Byun, D.W., Novak, J.H., Galluppi, K.J., Coats, C.J., Vouk, M.A., 1996. The next generation of integrated air quality modeling: EPA's models-3. Atmospheric Environment 30 (12), 1925–1938.

Dhaniyala, S., Wexler, A.S., 1996. Numerical schemes to model condensation and evaporation of aerosols. Atmospheric Environment 30 (6), 919–928.

Eldering, A., Cass, G.R., 1996. Source-oriented model for air pollutant effects on visibility. Journal of Geophysical Research 101 (D14), 19343–19369.

Gelbard, F., Tambour, Y., Seinfeld, J.H., 1980. Sectional representations for simulating aerosol dynamics. Journal of Colloid and Interface Science 76, 541–556.

Heintzenberg, J., 1989. Fine particles in the global troposphere: a review. Tellus 41B, 149–160.

Hughes, L.S., Allen, J.O., Kleeman, M.J., Johnson, R.J., Cass, G.R., Gross, D.S., Gard, E.E., Gaelli, M.E., Morrical, B.D., Fergenson, D.P., Dienes, T., Noble, C.A., Liu, D.-Y., Silva, P.J., Prather, K.A., 1999. Size and composition distribution of atmospheric particles in Southern California. Environmental Science and Technology 33 (20), 3506–3515.

Jacobson, M.Z., 1997. Development and application of a new air pollution modeling system. 2. Aerosol module structure and design. Atmospheric Environment 31 (2), 131–144.

Kleeman, M.J., Cass, G.R., Eldering, A., 1997. Modeling the airborne particle complex as a source-oriented external mixture. Journal of Geophysical Research-Atmospheres 102 (D17), 21355–21372.

Magliano, K.L., Hughes, V.M., Chinkin, L.R., Coe, D.L., Haste, T.L., Kumar, N., Lurmann, F.W., 1999. Spatial and temporal variations in PM10 and PM2.5 source contributions and comparison to emissions during the 1995 integrated monitoring study. Atmospheric Environment 33 (29), 4757–4773.

Morris, R.E., Yarwood, G., Emery, C., Pandis, S., Lurmann, F., 2003. Implementation of state-of-science PM modules into the PMCAMx photochemical grid model. In: Proceedings of the 96th Annual Conference and Exhibition of the A&WMA, San Diego, CA. Available from: 〈www.camx.com〉.

NAS, 2004. Research priorities for airborne particulate matter. IV. Continuing research progress. Committee on Research Priorities for Airborne Particulate Matter, Board on Environmental Studies and Toxicology, Division on Earth and Life Studies, National Research Council of the National Academies. National Academies Press, Washington, DC.

Nenes, A., Pandis, S.N., Pilinis, C., 1998. ISORROPIA: a new thermodynamic equilibrium model for multiphase multicomponent inorganic aerosols. Aquatic Geochemistry 4 (1), 123–152.

Nolte, C.G., Bhave, P.V., Dennis, R.L., Arnold, J.R., Zhang, K.M., Wexler, A.S., 2008. Modeling of urban and regional aerosols—Application of the CMAQ-UCD Aerosol Model to Tampa, a coastal urban site. Atmospheric Environment 42, 3179–3191, this issue.

Pilinis, C., Seinfeld, J.H., 1988. Development and evaluation of an eulerian photochemical gas aerosol model. Atmospheric Environment 22 (9), 1985–2001.

Pilinis, C., Capaldo, K.P., Nenes, A., Pandis, S.N., 2000. MADM—a new multicomponent aerosol dynamics model. Aerosol Science and Technology 32 (5), 482–502.

Potukuchi, S., Wexler, A.S., 1995a. Identifying solid–aqueous phase transitions in atmospheric aerosols: I. Neutral-acidity solutions. Atmospheric Environment 29, 1663–1676, 1995.

Potukuchi, S., Wexler, A.S., 1995b. Identifying solid–aqueous phase transitions in atmospheric aerosols: II. Acidic solutions. Atmospheric Environment 29, 3357–3364, 1995.

Stelson, A.W., Seinfeld, J.H., 1982. Relative humidity and pH dependence of the vapor pressure of ammonium nitrate–nitric acid solutions at 25 degrees C. Atmospheric Environment 16, 993–1000.

Stokes, R.H., Robinson, R.A., 1966. Interactions in aqueous nonelectrolyte solutions: I. Solute–solvent equilibria. Journal of Physical Chemistry 70, 2126–2130.

Sun, Q., 1999. Modeling urban and regional aerosols. Ph.D. Thesis, Department of Mechanical Engineering, University of Delaware.

Sun, Q., Wexler, A.S., 1998a. Modeling urban and regional aerosols—condensation and evaporation near acid neutrality. Atmospheric Environment 32 (20), 3527–3531.

Sun, Q., Wexler, A.S., 1998b. Modeling urban and regional aerosols near acid neutrality—application to the June 24–25 SCAQS episode. Atmospheric Environment 32, 3533–3545.

Wagman, D.D., Evans, W.H., Parker, V.B., Schumm, R.H., Halow, I., Bailey, S.M., Churney, K.L., Nuttall, R.L., 1982. The NBS tables of chemical thermodynamic properties—selected values for inorganic and C-1 and C-2 organic-substances in SI units. Journal of Physical and Chemical Reference Data 11 (Suppl. 2).

Wexler, A.S., Clegg, S.L., 2002. Atmospheric aerosol models for systems including the ions H^+, NH_4^+, Na^+, SO_4^{2-}, NO_3^-, Cl^-, Br^-, and H_2O. Journal of Geophysical Research-Atmospheres 107 (D14) (art. no. 4207).

Wexler, A.S., Potukuchi, S., 1998. Kinetics and thermodynamics of tropospheric aerosols. In: Harrison, R.M., Van Grieken, R. (Eds.), Atmospheric Particles. Wiley.

Wexler, A.S., Seinfeld, J.H., 1990. The distribution of ammonium salts among a size and composition dispersed aerosol. Atmospheric Environment 24A (5), 1231–1246.

Wexler, A.S., Seinfeld, J.H., 1991. Second-generation inorganic aerosol model. Atmospheric Environment 25A (5), 2731–2748.

Wexler, A.S., Lurmann, F.W., Seinfeld, J.H., 1994. Modeling urban and regional aerosols—I. Model development. Atmospheric Environment 28 (3), 531–546.

Zhang, K.M., Wexler, A.S., 2006. An Asynchronous Time-Stepping (ATS) integrator for atmospheric applications—aerosol dynamics. Atmospheric Environment 40 (24), 4574–4588.

Zhang, Y., Pun, B., Vijayaraghavan, K., Wu, S.Y., Seigneur, C., Pandis, S.N., Jacobson, M.Z., Nenes, A., Seinfeld, J.H., 2004. Development and application of the model of aerosol dynamics, reaction, ionization, and dissolution (MADRID). Journal of Geophysical Research-Atmospheres 109 (D1) (art. no. D01202).